

Article

Antioxidant Activities of Plant Extracts (*Ammannia multiflora*, *Ammannia coccinea*, and *Salix gracilistyla*) Activate the Nrf2/HO-1 Signaling Pathway

Jayasingha Arachchige Chathuranga Chanaka Jayasingha ¹, Yung Hyun Choi ² , Chang-Hee Kang ³, Mi-Hwa Lee ³, Moon-Soo Heo ^{1,*} and Gi-Young Kim ^{1,*} 

¹ Department of Marine Life Science, Jeju National University, Jeju 63243, Republic of Korea; chanakajayasinghe7@gmail.com

² Department of Biochemistry, College of Korean Medicine, Dong-Eui University, Busan 47227, Republic of Korea; choiyh@deu.ac.kr

³ Nakdonggang National Institute of Biological Resources, Sangju 37242, Republic of Korea; ckdgml3735@nnibr.re.kr (C.-H.K.); blume96@nnibr.re.kr (M.-H.L.)

* Correspondence: msheo@jejunu.ac.kr (M.-S.H.); immunkim@jejunu.ac.kr (G.-Y.K.)

Abstract: To identify potent plant extracts with strong antioxidant activity, we evaluated the free radical scavenging activity of 184 plant extracts obtained from the Freshwater Bioresources Culture Collection (FBCC) of Nakdonggang National Institute of Biological Resources (Republic of Korea), as various plant extracts have been used therapeutically to prevent chronic diseases associated with oxidative stress. From them, three plant extracts (FBCC-EP858 from *Ammannia multiflora*, FBCC-EP920 from *Ammannia coccinea*, and FBCC-EP1014 from *Salix gracilistyla*) were selected based on their abilities to scavenge the 2,2-diphenyl-1-picrylhydrazyl (DPPH) radical with more than 80% efficiency. We found that these extracts had in vitro half maximal inhibitory concentration (IC₅₀) values ranging from 11.89 to 14.26 µg/mL and strong total antioxidant activity (corresponding to approximately 0.18, 0.22, and 0.23 mM Trolox, respectively). We also studied the effect of these extracts on RAW 264.7 macrophages and found that FBCC-EP920 significantly downregulated relative cell viability at a concentration of 100 µg/mL. However, the other two extracts, FBCC-EP858 and FBCC-EP1014, did not affect cell viability at the same concentration. Additionally, all three extracts inhibited hydrogen peroxide (H₂O₂)-induced reactive oxygen species (ROS) production and depolarization of mitochondrial membrane potential in RAW 264.7 macrophages. An additional experiment in zebrafish larvae showed that the three extracts reduced 2',7'-dichlorodihydrofluorescein diacetate (DCFDA) fluorescent intensity induced by H₂O₂. The extracts also upregulated the expression of nuclear factor erythroid 2-related factor 2 (Nrf2) and heme oxygenase-1 (HO-1) expression, and an HO-1 inhibitor, zinc protoporphyrin (ZnPP), attenuated the extract-induced antioxidant activity both in vivo and in vitro. Taken together, these findings suggest that the extracts from *A. multiflora*, *A. coccinea*, and *S. gracilistyla* have potential free radical scavenging and antioxidant capacities both in vivo and in vitro by activating the Nrf2/HO-1 signaling pathway. These results could be useful for the prevention and treatment of various oxidative stress-mediated human diseases.

Keywords: RAW 264.7 macrophages; zebrafish larvae; H₂O₂; ROS; bioactive activity



Citation: Jayasingha, J.A.C.C.; Choi, Y.H.; Kang, C.-H.; Lee, M.-H.; Heo, M.-S.; Kim, G.-Y. Antioxidant Activities of Plant Extracts (*Ammannia multiflora*, *Ammannia coccinea*, and *Salix gracilistyla*) Activate the Nrf2/HO-1 Signaling Pathway. *Appl. Sci.* **2023**, *13*, 6701. <https://doi.org/10.3390/app13116701>

Academic Editors: Antony C. Calokerinos and Roger Narayan

Received: 5 April 2023

Revised: 27 April 2023

Accepted: 26 May 2023

Published: 31 May 2023



Copyright: © 2023 by the authors. Licensee MDPI, Basel, Switzerland. This article is an open access article distributed under the terms and conditions of the Creative Commons Attribution (CC BY) license (<https://creativecommons.org/licenses/by/4.0/>).

1. Introduction

Oxidative stress induced by excessive reactive oxygen species (ROS) contributes to inflammatory diseases and metabolic syndromes, including vascular and neurodegenerative diseases and various cancers [1,2]. Specifically, aberrant ROS production causes cellular lipid oxidation and DNA damage, which affect cellular malfunction in cell division and differentiation, ion-homeostasis, regulation of apoptosis, and inflammation [3,4]. To maintain homeostasis of ROS levels, several antioxidant systems and agents are present

in our body; however, ROS production that exceeds antioxidant capacity causes physiological and pathological damage to cells [5,6]. Among antioxidant mechanisms, nuclear factor erythroid 2-related factor 2 (Nrf2) is an extremely crucial regulator that controls the antioxidant response element (ARE), resulting in the transcriptional activation of phase II detoxification and antioxidant enzymes, including heme oxygenase-1 (HO-1). In the absence of oxidative stress, Nrf2 forms a complex with Kelch-like epichlorohydrin-related proteins (Keap1) in the cytoplasm and exists with low activity in a state bound to actin [7,8]. Under physiological and pathological stress, such as excessive ROS production, modification of the cysteine residue of Keap1 releases Nrf2 through its conformational change and phosphorylation. This complex forms a complex with Maf protein to translocate into the nucleus and binds to AREs [9]. Then, Nrf2 initiates transcriptional activation of phase II detoxification and antioxidant enzymes, such as HO-1 and NAD(P)H:quinone oxidoreductase, resulting in the stimulation of cellular protective mechanisms against oxidative stress [10]. Therefore, pharmacological activators or agonists of Nrf2 are a promising strategy for oxidative stress-induced inflammatory diseases such as neurodegenerative, cardiovascular, and autoimmune diseases. Yagishita et al. recently demonstrated that Nrf2 is an excellent biomarker in the maintenance of cellular redox and metabolic homeostasis, and some Nrf2 activators, including dimethyl fumarate, bardoxolone methyl, oltipraz, and sulforaphane, are clinical compounds in humans [11]. Furthermore, some Nrf2 agonists are in clinical trials to investigate the therapeutic effects in various inflammation and age-related diseases such as rheumatoid arthritis, Alzheimer's disease (AD), Parkinson's disease (PD), lupus erythematosus (LE), and liver damage [12]. In addition, Nrf2 deficiency favors the carcinogenesis of many different types of cancers [13], and phytochemicals targeting the Nrf2/HO-1 pathway reduce excessive carcinogenic metabolites and inhibit carcinogenesis [14,15]. Therefore, the discovery of novel Nrf2 activators or agonists has the nutritional potential to inhibit inflammatory diseases.

Plant-derived extracts and products are widely recognized for their potential as functional foods and traditional medicines due to their rich content of bioactive compounds with significant health benefits. These compounds have been shown to target various pathophysiological conditions, such as oxidative stress, aging, lipid oxidation, diabetes, gut inflammation, and cancer progression [16]. Additionally, plant-derived antioxidants may have an enhanced therapeutic potential due to their ability to reduce toxicity and inhibit the pathophysiological hallmarks of many human diseases by reducing oxidative stress [17,18]. In proving the potential antioxidative activity related to the human disease models, zebrafish larvae have been a very promising technique to evaluate the overall performance of the agent which is being tested. The zebrafish model has been beneficial in human disease models or drug screening due to the shorter-timed response from larvae and the advantages of the smaller size of larvae, facilitating more accurate average data [19]. Numerous studies have demonstrated the effectiveness of natural antioxidants in treating oxidative stress-mediated inflammatory and metabolic diseases by activating the Nrf2-HO-1 signaling pathway [20].

Ammannia multiflora is a plant belonging family Lythraceae and is well-known as an annual dicot weedy plant in agricultural lands and plants inhabiting aquatic environmental systems [21]. According to studies over the years, it has been proven that *A. multiflora* contains medicinal properties as it has shown antihyperglycemic activity, antimalarial properties, and microbicidal properties [21–25]. Regarding the biochemical and phytochemical analysis, the studies have revealed that it is rich in flavonoids, which may contribute to antioxidant activity [26]. *Ammannia coccinea* is a semi-aquatic, marsh-inhabiting plant and is geographically distributed in both temperate and tropical zones as well as near the mountains [27]. In the recent literature, medicinal properties of *Ammannia* sp. are reported [26]. *Salix gracilistyla* is a plant inhabiting riverbanks and streams [28]. Regarding the therapeutic properties, it has been recorded that it exhibits antioxidants and whitening activities [29], possessing α -Amylase inhibitor activity, with a higher percentage [30]. Additionally, an

extensive study on their antioxidative activities with detailed molecular mechanisms has not been conducted yet.

In this study, we aimed to identify plant-derived strong antioxidant extracts by screening 184 plant extracts obtained from the Freshwater Bioresources Culture Collection (FBCC) at the Nakdonggang National Institute of Biological Resources (NNIBR) located in Sangju, Gyeongsangbuk-do, Republic of Korea. After evaluation, we selected three extracts with strong 2,2-diphenyl-1-picrylhydrazyl (DHPH) radical scavenging activity, namely *Ammannia multiflora* Rehder (FBCC-EP858), *Ammannia coccinea* Makino (FBCC-EP920), and *Salix gracilistyla* Maq. (FBCC-EP1014). Subsequently, we investigated possessing the antioxidant activity and activation of Nrf2 of three extracts investigated in hydrogen peroxide (H₂O₂)-treated RAW 264.7 macrophages and zebrafish larvae.

2. Materials and Methods

2.1. Plant-Derived Extracts

All extracts used in this study (FBCC-EP844~FBCC-EP869, FBCC-EP871~FBCC-EP873, FBCC-EP875~FBCC-EP879, FBCC-EP881~FBCC-EP910, FBCC-EP912~FBCC-EP928, FBCC-EP1013~FBCC-EP1036, FBCC-EP1038~FBCC-EP1042, FBCC-EP1044~FBCC-EP1057, FBCC-EP1059~FBCC-EP1082, FBCC-EP1084~FBCC-EP1093, and FBCC-EP1095~FBCC-EP1116) were provided by NNIBR (Supplementary Table S1). Briefly, a total of 184 plants were extracted, either in part or in their entirety, using 70% ethanol or distilled water. To prepare the ethanolic extracts, 3 kg of the plant materials were macerated and extracted twice in 50 L of 70% (v/v) ethanol (Daejung, Busan, Republic of Korea) for two days (d) at room temperature. The resulting mixture was then filtered through ADVANTEC no. 2 filter paper (ADVANTEC, Tokyo, Japan), and the ethanol in the crude extracts was removed using a rotary vacuum evaporator (Eyela, Tokyo, Japan) at 37 °C until it was fully dried. For the aqueous extract, 1 kg of the plant materials was macerated and extracted twice in 10 L of distilled water for 3 d at 100 °C, then filtered through ADVANTEC no. 2 filter paper. The aqueous extract was completely dried using a vacuum freeze dryer (Operon, Gimpo, Republic of Korea). Finally, the extract powders were dissolved in dimethyl sulfoxide (DMSO, Sigma–Aldrich, St. Louis, MO, USA) at a concentration of 20 mg/mL. From these extracts, three extracts (FBCC-EP858, FBCC-EP920, and FBCC-EP1014) exhibiting strong 2,2-diphenyl-1-picrylhydrazyl (DPPH) radical scavenging activities were selected.

2.2. Reagents and Antibodies

Dulbecco's Modified Eagle's Medium (DMEM), fetal bovine serum (FBS), and antibiotic mixture were obtained from WELGENE (Gyeongsan, Gyeongsangbuk-do, Republic of Korea). The 2',7'-Dichlorodihydrofluorescein diacetate (DCFDA), DPPH, and zinc protoporphyrin (ZnPP) were purchased from Sigma–Aldrich. A WST-8 assay kit was purchased from MediFab (Seoul, Republic of Korea), and an OxiTec Total Antioxidant Capacity Assay Kit was purchased from BIOMAX (Guri, Gyeonggi-do, Republic of Korea). Antibodies against Nrf2 (sc-365949, 60 kDa), HO-1 (sc-136960, 32 kDa), β -actin (sc-69879, 43 kDa), and peroxidase-labeled anti-mouse immunoglobulins (sc-16102) were purchased from Santa Cruz Biotechnology (Dallas, TX, USA).

2.3. DPPH Radical Scavenging Assay

DPPH radical scavenging activity was measured by testing three extracts (FBCC-EP858, FBCC-EP920, and FBCC-EP1014) and comparing them to the positive control, which was 20 μ M ascorbic acid. Briefly, 120 μ M DPPH in 95% ethyl alcohol was freshly prepared, and then 190 μ L DPPH was mixed with 10 μ L each extract (ranging from 0 to 100 μ g/mL) at room temperature for 10 min. The absorbance value was then measured at the wavelength of 517 nm (BioTek Instruments, Inc., Winooski, VT, USA). The half maximal inhibitory concentration (IC₅₀) was calculated using GraphPad Prism 9 software (GraphPad Software, Boston, MA, USA).

2.4. Total Antioxidant Capacity

The reduction rate of Cu^{2+} was measured using an OxiTec Total Antioxidant Capacity Assay Kit, with Trolox as the standard for comparison. Briefly, 100 μL reaction buffer and 100 μL copper reagent were mixed and then treated with 100 μL each extract (ranging from 0 to 100 $\mu\text{g}/\text{mL}$) for 30 min at room temperature. A standard curve of Trolox was prepared, and the concentration of the extract was calculated corresponding to Trolox concentration. Ascorbic acid (400 μM) was used as a representative antioxidant positive control. For the blank control, the reaction buffer was replaced with ethanol. Each solution (120 μL) was transferred to a 96-microplate, and the absorbance was read at a wavelength of 450 nm.

2.5. Cell Culture and Relative Cell Viability

RAW 264.7 macrophages were obtained from the American Type Culture Collection (ATCC, Manassas, VA, USA) and cultured in DMEM supplemented with 5% FBS at 37 °C in 5% CO_2 . The cells were seeded at a density of 5×10^4 cells/mL, and cell viability was determined using a WST-8 (highly sensitive water-soluble tetrazolium salt) Viability Assay Kit. Briefly, RAW 264.7 macrophages were treated with various concentrations (0–100 $\mu\text{g}/\text{mL}$) of each extract. After a 24 h incubation, 10 μL of WST-8 solution was added to the cell culture media and incubated for 1 h. Absorbance was measured at a wavelength of 450 nm (BioTek Instruments, Inc.).

2.6. Flow Cytometry Analysis

RAW 264.7 macrophages (5×10^4 cells/mL) were treated with various concentrations (0–100 $\mu\text{g}/\text{mL}$) of FBCC-EP858 and FBCC-EP1014 for 20 h and 200 μM H_2O_2 treated for 4 h. The maximum concentration of FBCC-EP920 was set at 50 $\mu\text{g}/\text{mL}$ since a concentration of 100 $\mu\text{g}/\text{mL}$ resulted in a slight decrease in relative cell viability.

2.6.1. ROS Production

Cellular ROS production was analyzed using a Muse Oxidative Stress Kit (Luminex, Austin, TX, USA). Briefly, cells were suspended in $1 \times$ assay buffer and incubated at 37 °C for 30 min. Cells exhibiting ROS (ROS^+) were then analyzed using a Muse Cell Analyzer (Luminex) [31].

2.6.2. Depolarization of Mitochondrial Membrane Potential

Depolarization of mitochondrial membrane potential was measured using a Muse MitoPotential Kit (Luminex). Briefly, cells were suspended in $1 \times$ assay buffer and mixed thoroughly with MitoPotential working solution. The cells were incubated at 37 °C for 20 min, and MitoPotential 7-ADD reagent was added for 5 min at room temperature. Cells exhibiting depolarized mitochondrial membrane potential were finally measured using a Muse Cell Analyzer [32].

2.7. Reverse-Transcription Polymerase Chain Reaction (RT-PCR)

RAW 264.7 macrophages were treated with various concentrations of each extract. Total RNA was extracted using an Easy-BLUE Total RNA Extraction Kit (iNtRON Biotechnology, Sungnam, Gyeonggi-do, Republic of Korea). The RNA was reverse transcribed using MMLV reverse transcriptase (Bioneer, Daejeon, Republic of Korea), and target genes were amplified using specific primers (Table 1) [33].

Table 1. Primer sequences for RT-PCR used in this study.

Gene ⁽¹⁾	Primer Sequence (5'→3')	Size ⁽²⁾	Gene Accession No.
<i>Nrf2</i>	F: 5'-TGGACGGGACTATTGAAGGC-3' R: 5'-GCCGCCTTTTCAGTAGATGG-3'	735 bp	NM_010902.5
<i>HO-1</i>	F: 5'-TGAAGGAGGCCACCAAGGAG-3' R: 5'-AGAGGTCACCCAGGTAGCGG-3'	375 bp	NM_010442.2
<i>GAPDH</i>	F: 5'-ACCACAGTCCATGCCATCAC-3' R: 5'-CACCACCCTGTTGCTGTAGC-3'	450 bp	NM_001411843.1

⁽¹⁾ *Nrf2*, nuclear factor erythroid 2-related factor 2; *HO-1*, heme oxygenase-1; *GAPDH*, glyceraldehyde 3-phosphate dehydrogenase. ⁽²⁾ bp, base pairs.

2.8. Western Blotting

Total cellular proteins were prepared using RIPA Lysis Buffer (ROCKLAND, Pottstown, PA, USA) with protease inhibitors (Thermo Fisher Scientific, Rockford, IL, USA). Protein concentration was determined using a Bio-Rad Protein Assay Kit (Bio-Rad, Hercules, CA, USA), and an equal amount of protein (20 µg) was loaded on a 10% sodium dodecyl sulfate-polyacrylamide gel and transferred onto a polyvinylidene difluoride membrane (Thermo Fisher Scientific). The membrane was incubated with primary and secondary antibodies and developed using a SuperSignal West Femto Maximum Sensitivity Substrate (Thermo Fisher Scientific) [34].

2.9. Measurement of ROS Production in Zebrafish Larvae

Animal Care and Use Committee of Jeju National University (Jeju Special Self-governing Province, Republic of Korea) approved a zebrafish study for DCFDA staining (Approval No. 2022-0084). All zebrafish experiments followed the approval guidelines described previously [35]. In this experiment, zebrafish larvae were used to investigate the effects of each extract on ROS production. Zebrafish at three days post fertilization (dpf) were treated with each extract for 2 h before being treated with 1 mM H₂O₂ for 22 h. Then, the zebrafish were stained with 20 µM DCFDA for 30 min and visualized using a CELENA S Digital Imaging System (Logos Biosystems, Anyang, Gyeonggi-do, Republic of Korea). In a parallel experiment, an HO-1 inhibitor, ZnPP, was used to evaluate HO-1-mediated antioxidant activity. Each extract was incubated for 2 h, followed by treatment with ZnPP for 1 h, and then 1 mM H₂O₂ for 22 h.

2.10. Statistical Analysis

The western blots and RT-PCR results were quantified using ImageJ 1.50i (National Institute of Health, Bethesda, MD, USA, www.imagej.net, accessed on 22 July 2022), and all data were analyzed using SigmaPlot version 12.5 (Systat Software, San Jose, CA, USA, www.systatsoftware.com, accessed on 28 July 2022). The data represent the mean of at least three independent experiments, and significant differences were determined using Student's *t*-test and an unpaired one-way ANOVA test with Bonferroni correction. The significance levels are denoted by different symbols (###, ***, and +++ *p* < 0.001, ## and ** *p* < 0.01, and * *p* < 0.05).

3. Results

3.1. FBCC-EP858, FBCC-EP920, and FBCC-EP1014 Exhibit Strong DPPH Radical Scavenging Activity

To identify potent antioxidant extracts from plants, we screened 184 extracts obtained from various plants found in the Nakdong River basin in the Republic of Korea, obtained from NNIBR, for their DPPH radical scavenging activity. Approximately 32% of the extracts exhibited DPPH radical scavenging activity of 50% or more at a concentration of 50 µg/mL (Supplementary Table S1), and among these, FBCC-EP858, FBCC-EP920, and FBCC-EP1014 exhibited DPPH radical scavenging capacity of over 80%. We further

investigated the concentration-dependent DPPH radical scavenging activity and total antioxidant activity of these three extracts *in vitro*. The extracts demonstrated strong DPPH radical scavenging activity in a concentration-dependent manner (Table 2), with FBCC-EP858, FBCC-EP920, and FBCC-EP1014 exhibiting IC_{50} values of 13.75 $\mu\text{g/mL}$, 14.26 $\mu\text{g/mL}$, and 11.89 $\mu\text{g/mL}$, respectively (Figure 1). The three extracts also exhibited strong total antioxidant capacity (Table 1), with FBCC-EP1014 exhibiting the strongest total antioxidant capacity, corresponding to 0.0003 ± 0.0017 , 0.0890 ± 0.0010 , 0.1080 ± 0.0010 , 0.1550 ± 0.0003 , 0.2270 ± 0.0027 , and 0.4300 ± 0.0020 mM Trolox at 0, 6.25, 12.5, 25, 50, and 100 $\mu\text{g/mL}$, respectively. FBCC-EP858 showed total antioxidant capacity, corresponding to 0.0523 ± 0.0037 , 0.0803 ± 0.0007 , 0.1160 ± 0.0003 , 0.1180 ± 0.0033 , 0.1830 ± 0.0000 , and 0.2850 ± 0.0037 mM Trolox at 0, 6.25, 12.5, 25, 50, and 100 $\mu\text{g/mL}$, respectively (Table 2). FBCC-EP920 increased the capacity in a concentration-dependent manner, corresponding to 0.0600 ± 0.0010 , 0.0810 ± 0.0010 , 0.0883 ± 0.0017 , 0.1540 ± 0.0010 , 0.2150 ± 0.0003 , and 0.3860 ± 0.0013 mM Trolox. FBCC-EP1014 exhibited the strongest total antioxidant capacity; 0.0003 ± 0.0017 , 0.0890 ± 0.0010 , 0.1080 ± 0.0010 , 0.1550 ± 0.0003 , 0.2270 ± 0.0027 , and 0.4300 ± 0.0020 mM at 0, 6.25, 12.5, 25, 50, and 100 $\mu\text{g/mL}$, respectively. At a concentration of 12.5 $\mu\text{g/mL}$, the three extracts had total antioxidant activity similar to that of 400 μM ascorbic acid, which is equivalent to 0.1 mM Trolox. These findings suggest that FBCC-EP858, FBCC-EP920, and FBCC-EP1014 are potent plant-derived antioxidants.

Table 2. *In vitro* DPPH radical scavenging activity and total antioxidant activity of three extracts used in this study.

FBCC No.	Con. ($\mu\text{g/mL}$)	DPPH Radical Scavenging Activity (%)	Total Antioxidant Activity (Trolox Con., mM)
FBCC-EP858	0	3.7 ± 0.4	0.0523 ± 0.0037
	6.25	30.4 ± 0.1	0.0803 ± 0.0007
	12.5	48.5 ± 1.3	0.1160 ± 0.0003
	25	69.3 ± 2.2	0.1180 ± 0.0033
	50	84.6 ± 2.3	0.1830 ± 0.0000
	100	94.0 ± 0.3	0.2850 ± 0.0037
FBCC-EP920	0	03.9 ± 0.5	0.0600 ± 0.0010
	6.25	26.4 ± 2.6	0.0810 ± 0.0010
	12.5	47.2 ± 1.8	0.0883 ± 0.0017
	25	68.4 ± 3.3	0.1540 ± 0.0010
	50	82.5 ± 2.3	0.2150 ± 0.0003
	100	94.1 ± 1.7	0.3860 ± 0.0013
FBCC-EP1014	0	3.7 ± 0.5	0.0003 ± 0.0017
	6.25	31.5 ± 0.8	0.0890 ± 0.0010
	12.5	49.2 ± 1.1	0.1080 ± 0.0010
	25	67.4 ± 4.2	0.1550 ± 0.0003
	50	87.0 ± 1.3	0.2270 ± 0.0027
	100	88.2 ± 0.3	0.4300 ± 0.0020
Ascorbic acid	20 ⁽¹⁾ or 400 ⁽²⁾ μM	53.8 ± 0.3	0.1010 ± 0.0003

⁽¹⁾ DPPH radical scavenging activity. ⁽²⁾ Total antioxidant activity.

3.2. FBCC-EP858, FBCC-EP920, and FBCC-EP1014 Regulate the Viability of RAW 264.7 Macrophages Depending on Their Concentrations

Prior to evaluating the cellular antioxidant activity of FBCC-EP858, FBCC-EP920, and FBCC-EP1014, the relative viability of RAW 264.7 cells was assessed using the WST-8 assay. As depicted in Figure 2, FBCC-EP858 and FBCC-1014 did not exhibit any significant effect on cell morphology or relative cell viability. However, FBCC-EP920 at a concentration of 100 $\mu\text{g/mL}$ decreased the cell number (Figure 2A) and relative cell viability ($85.0 \pm 3.2\%$, Figure 2B). For further investigation, FBCC-EP920 was used at a maximum concentration of 50 $\mu\text{g/mL}$, while the highest concentration of FBCC-EP858 and FBCC-1014 was set at 100 $\mu\text{g/mL}$.

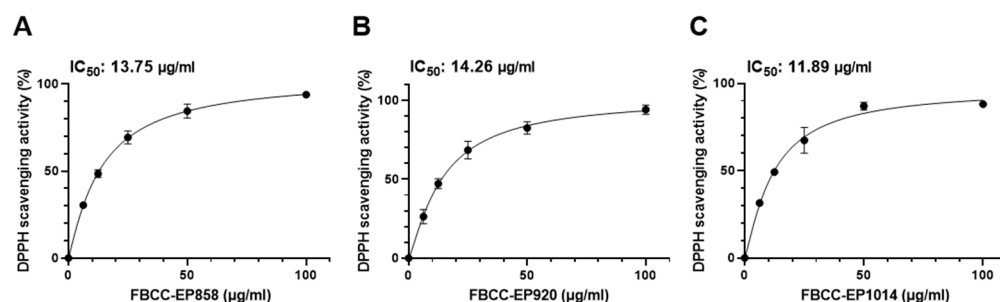


Figure 1. The IC₅₀ value of in vitro DPPH radical scavenging activity. The indicated concentrations (0–100 µg/mL) of FBCC-EP858, FBCC-EP920, and FBCC-EP1014 were mixed with DPPH solution for 10 min. Absorbance = 517 nm. (A–C) IC₅₀ was evaluated for each extract using DPPH scavenging activity (%).

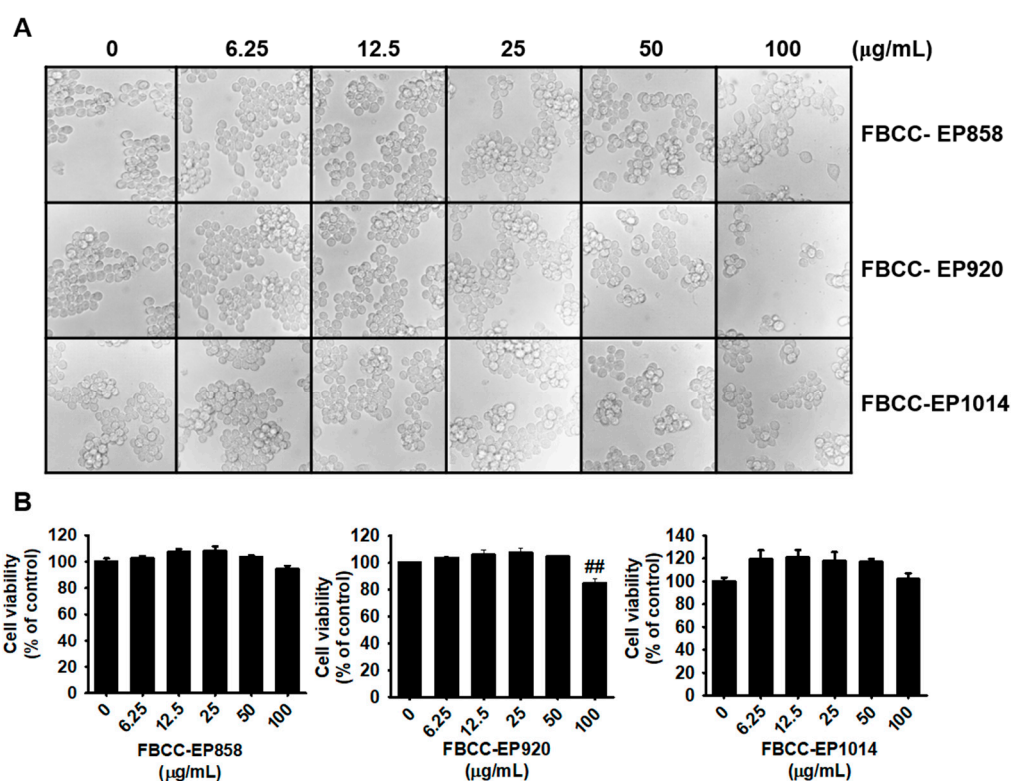


Figure 2. Relative cell viability. RAW 264.7 macrophages were seeded at a density of 1×10^4 cells/mL and treated with the indicated concentrations (0–100 µg/mL) of FBCC-EP858, FBCC-EP920, and FBCC-EP1014 for 24 h. (A) The cytotoxicity was evaluated morphologically using phase-contrast microscopy ($\times 10$). (B) The quantification of cell viability was conducted using WST-8 assay. Each value indicates the mean \pm SEM from three independent experiments. Significant differences among the groups were determined using an unpaired one-way ANOVA with Bonferroni correction. ## $p < 0.01$ vs. untreated cells.

3.3. FBCC-EP858, FBCC-EP920, and FBCC-EP1014 Alleviate H₂O₂-Induced ROS Production in RAW 264.7 Cells and Zebrafish Larvae

To evaluate the cellular antioxidant activity of FBCC-EP858, FBCC-EP920, and FBCC-EP1014, we investigated whether the extracts could downregulate ROS⁺ cell population in H₂O₂-exposed RAW 264.7 cells using flow cytometry. As shown in Figure 3A, the ROS⁺ cell population (red peaks) significantly increased in H₂O₂-treated RAW 264.7 cells, and treatment with FBCC-EP858, FBCC-EP920, and FBCC-EP1014 downregulated the ROS⁺ cell population in a concentration-dependent manner. At a maximum concentration, FBCC-EP858, FBCC-EP920, and FBCC-EP1014 dramatically attenuated the ROS⁺ cell population

from approximately 30.5% to $16.5 \pm 0.5\%$, $18.3 \pm 0.4\%$, and $17.5 \pm 0.8\%$, respectively (Figure 3B). We also measured the *in vivo* antioxidant activity of these extracts in H_2O_2 -treated zebrafish larvae using DCFDA staining. Treatment with H_2O_2 increased DCFDA fluorescence (green) in zebrafish larvae, and FBCC-EP858, FBCC-EP920, and FBCC-EP1014 gradually diminished the fluorescence intensity in a concentration-dependent manner (Figure 3C,D). The results indicate that FBCC-EP858, FBCC-EP920, and FBCC-EP1014 can attenuate H_2O_2 -induced ROS production both *in vitro* and *in vivo*.

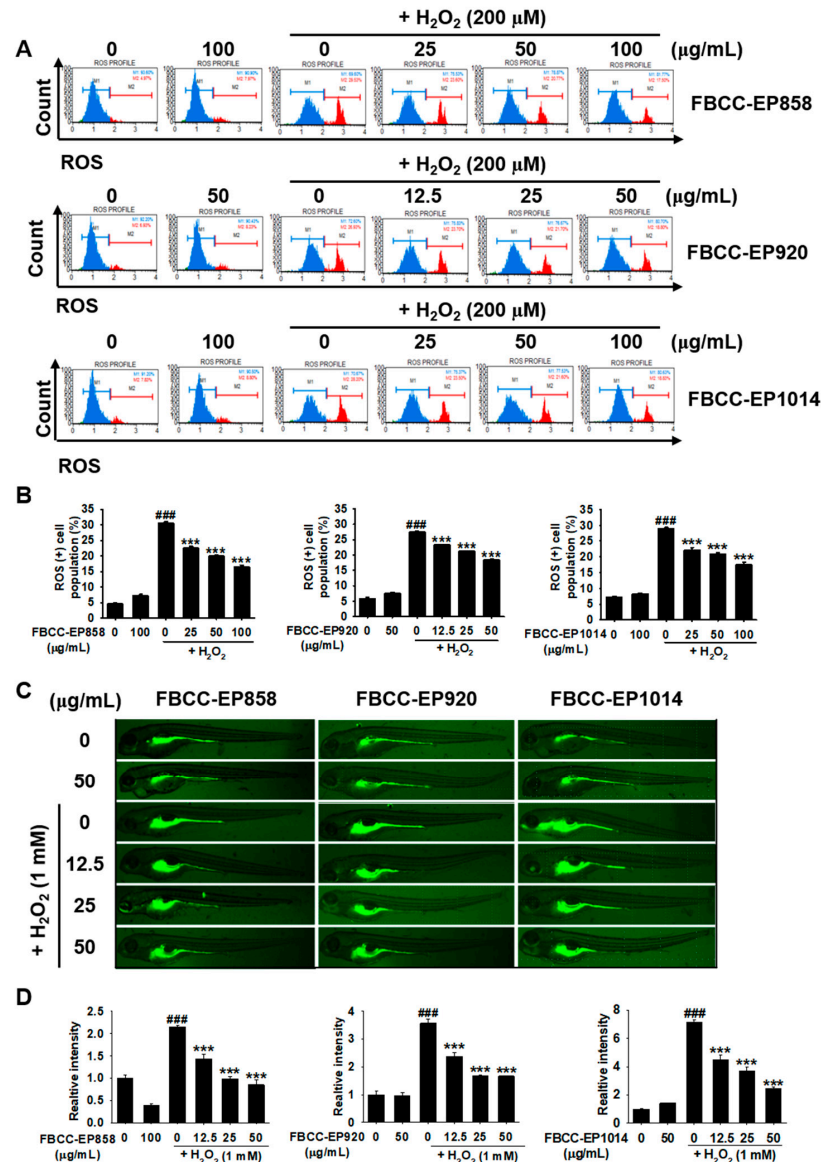


Figure 3. ROS production *in vitro* and *in vivo*. (**A,B**) RAW 264.7 macrophages were seeded at a density of 5×10^4 cells/mL and treated with the indicated concentrations of FBCC-EP858 (0–100 $\mu\text{g/mL}$), FBCC-EP920 (0–50 $\mu\text{g/mL}$), and FBCC-EP1014 (0–100 $\mu\text{g/mL}$) for 24 h, and 200 μM hydrogen peroxide (H_2O_2) was treated for 4 h. (**A**) The cells were stained using a Muse Oxidative Stress Kit, and (**B**) ROS^+ cell population was analyzed using a Muse Cell Analyzer. (**C,D**) The indicated concentrations of FBCC-EP858, FBCC-EP920, and FBCC-EP1014 were applied to 3 dpf zebrafish larvae 2 h before the addition of 1 mM H_2O_2 for 22 h. (**C**) The larvae were stained using 20 μM DCFDA for 30 min and visualized using a CELENA S Digital Imaging System. (**D**) The DCFDA fluorescence intensity was calculated using ImajJ 1.50i. Each value represents the mean \pm SEM from three independent experiments. Significant difference: ### $p < 0.001$ vs. untreated group (Student's *t*-test) and *** $p < 0.001$ vs. H_2O_2 -treated group (one-way ANOVA).

3.4. FBCC-EP858, FBCC-EP920, and FBCC-EP1014 Maintain Mitochondrial Membrane Potential in H₂O₂-Treated RAW 264.7 Macrophages

As oxidative stress is responsible for ROS-mediated cellular damage and depolarization of mitochondrial membrane potential [36], we investigated whether the reduction of ROS by FBCC-EP858, FBCC-EP920, and FBCC-EP1014 could preserve mitochondrial membrane potential in H₂O₂-treated RAW 264.7 cells. As illustrated in Figure 4A,B, H₂O₂ caused a significant increase in the total cell population with depolarized mitochondria membrane potential. However, treatment with FBCC-EP858, FBCC-EP920, and FBCC-EP1014 decreased the population and maintained mitochondrial membrane potential. These results suggest that FBCC-EP858, FBCC-EP920, and FBCC-EP1014 are able to prevent oxidative stress-induced depolarization of mitochondrial membrane potential.

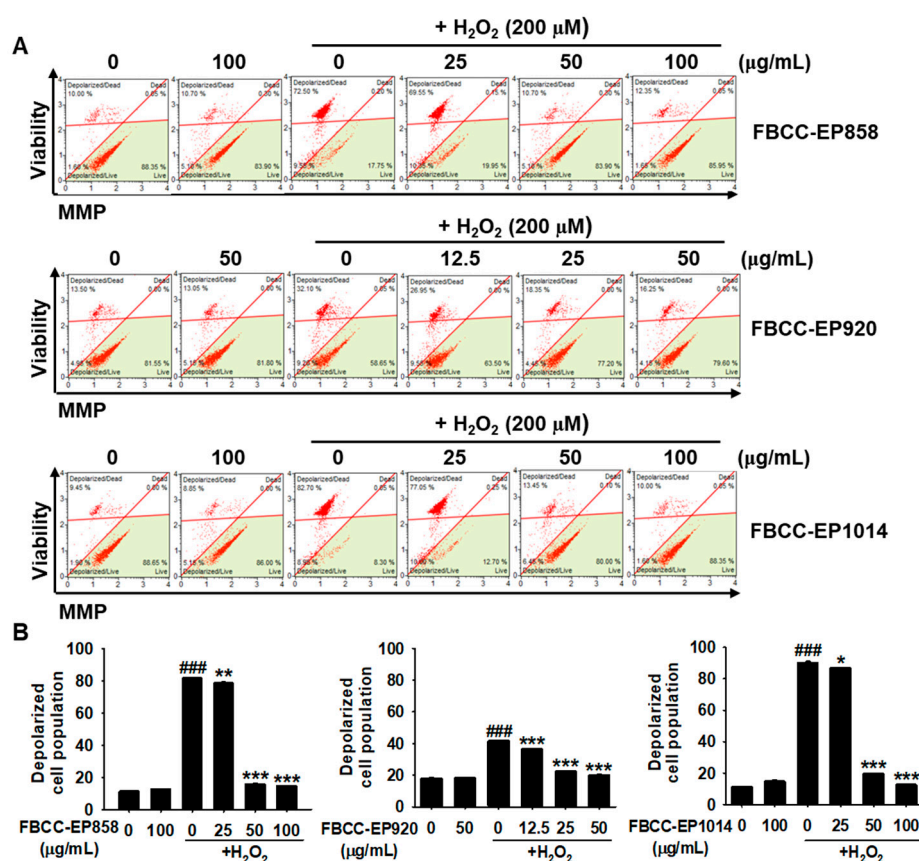


Figure 4. Mitochondrial membrane potential. RAW 264.7 macrophages were seeded at a density of 5×10^4 cells/mL and treated with the indicated concentrations of FBCC-EP858 (0–100 µg/mL), FBCC-EP920 (0–50 µg/mL), and FBCC-EP1014 (0–100 µg/mL) for 2 h followed by treatment with 200 µM H₂O₂ for 22 h. (A) The cells were stained using a Muse MitoPotential Kit, and (B) mitochondrial membrane depolarized cell population was analyzed using a Muse Cell Analyzer. Each value indicates the mean \pm SEM from three independent experiments. Significant difference: ### $p < 0.001$ vs. untreated cells (Student’s *t*-test), and *** $p < 0.001$, ** $p < 0.01$ and * $p < 0.05$ vs. H₂O₂-treated group (one-way ANOVA).

3.5. FBCC-EP858, FBCC-EP920, and FBCC-EP1014 Upregulate the Expression of Nrf2 and HO-1 in RAW 264.7 Macrophages

To confirm whether FBCC-EP858, FBCC-EP920, and FBCC-EP1014 can increase the expression of Nrf2 and HO-1, we performed RT-PCR and western blotting. Our results showed that treatment with FBCC-EP858 (Figure 5A), FBCC-EP920 (Figure 5B), and FBCC-EP1014 (Figure 5C) led to a concentration-dependent upregulation of Nrf2 and HO-1 expression in RAW 264.7 macrophages. Furthermore, consistent with gene expression data, FBCC-EP858 (Figure 6A), FBCC-EP920 (Figure 6B), and FBCC-EP1014 (Figure 6C) were

found to increase Nrf2 and HO-1 expression. These findings suggest that FBCC-EP858, FBCC-EP920, and FBCC-EP1014 can enhance Nrf2 and HO-1 expression.

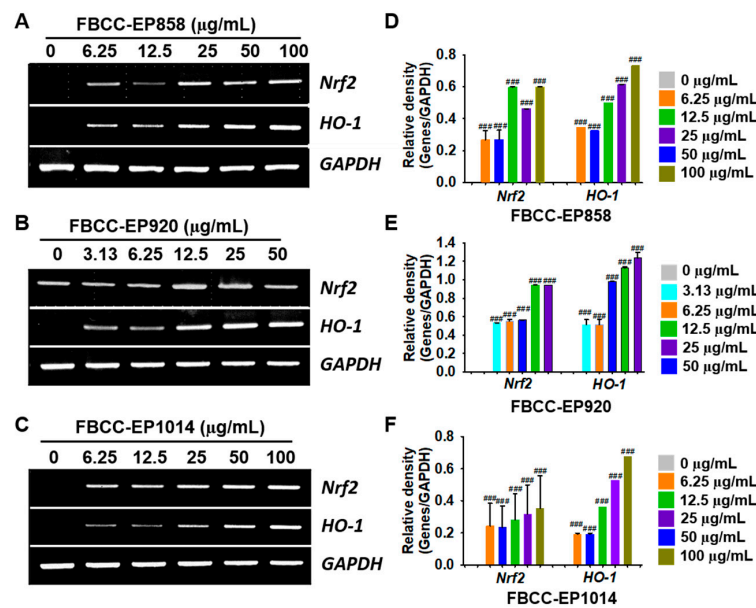


Figure 5. *Nrf2* and *HO-1* expression. RAW 264.7 macrophages were seeded at a density of 5×10^4 cells/mL and treated with (A) FBCC-EP858 (0–100 $\mu\text{g/mL}$), (B) FBCC-EP920 (0–50 $\mu\text{g/mL}$), and (C) FBCC-EP1014 (0–100 $\mu\text{g/mL}$) for 8 h. RNA was extracted and reverse-transcribed. After gene amplification, the amplicons were visualized using EtBr. *GAPDH* was used as the loading control. The amplicon intensity was calculated using ImageJ ((D), FBCC-EP858; (E), FBCC-EP920; (F), FBCC-EP1014). Each value indicates the mean \pm SEM from three independent experiments. Significant difference: ### $p < 0.001$ vs. untreated cells (one-way ANOVA).

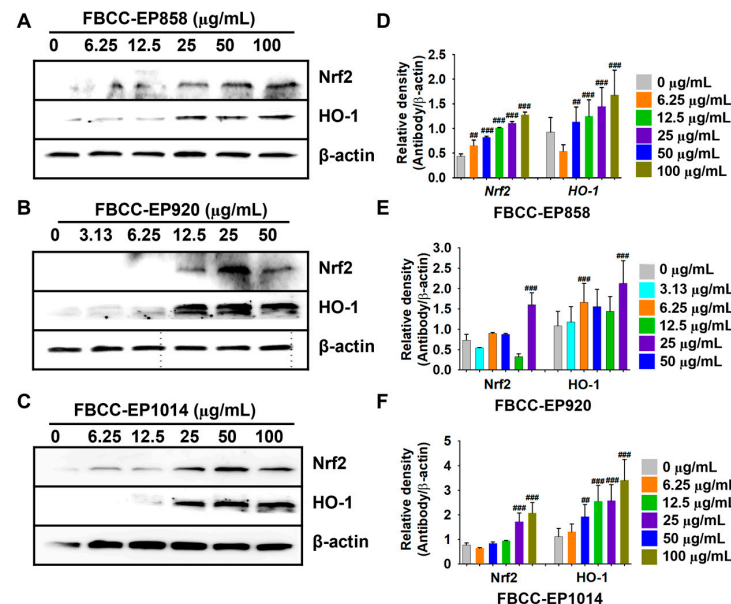


Figure 6. *Nrf2* and *HO-1* expression. RAW 264.7 macrophages were seeded at a density of 5×10^4 cells/mL and treated with (A) FBCC-EP858 (0–100 $\mu\text{g/mL}$), (B) FBCC-EP920 (0–50 $\mu\text{g/mL}$), and (C) FBCC-EP1014 (0–100 $\mu\text{g/mL}$) for 12 h. Total proteins were extracted, and western blotting was performed. β -Actin was used as the loading control. The band intensity was calculated using ImageJ ((D), FBCC-EP858; (E), FBCC-EP920; (F), FBCC-EP1014). Each value indicates the mean \pm SEM from three independent experiments. Significant differences: ### $p < 0.001$ and ## $p < 0.01$ vs. untreated cells (one-way ANOVA).

3.6. HO-1 Inhibition Reduces the Antioxidant Activity of FBCC-EP858, FBCC-EP920, and FBCC-EP1014

To confirm whether the reduction of ROS production by FBCC-EP858, FBCC-EP920, and FBCC-EP1014 is related to the activation of the Nrf2/HO-1 pathway, we investigated the effect of an HO-1 inhibitor, ZnPP, on ROS production. As shown in Figure 7A,B, H₂O₂ treatment increased the population of ROS⁺ cells, and treatment with FBCC-EP858, FBCC-EP920, and FBCC-EP1014 reduced the population (Figure 7A,B). However, treatment with ZnPP reversed the extract-induced reduction in the ROS⁺ cell population, causing an increase in the population. Additionally, DCFDA fluorescence intensity induced by H₂O₂ was significantly elevated in zebrafish larvae, and treatment with FBCC-EP858, FBCC-EP920, and FBCC-EP1014 attenuated the intensity (Figure 7C,D). Consistent with the data in Figure 7A,B, treatment with ZnPP reversed the three extract-induced reductions in DCFDA fluorescence intensity, causing a reversal increase. These results suggest that the antioxidant activity induced by FBCC-EP858, FBCC-EP920, and FBCC-EP1014 is related to the activation of the Nrf2/HO-1 pathway.

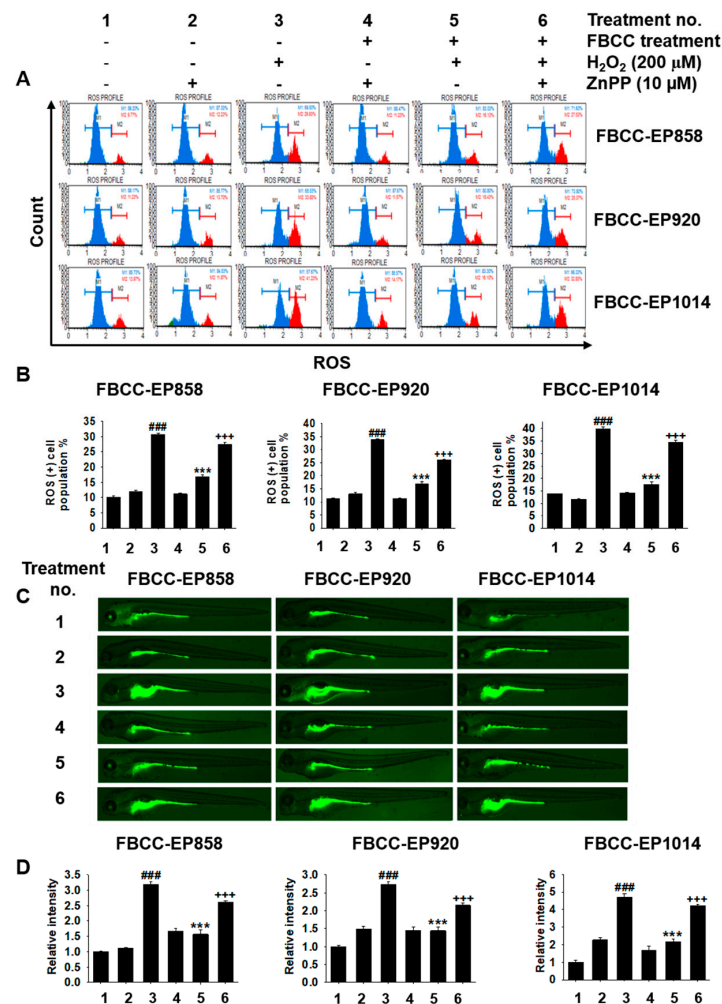


Figure 7. HO-1-mediated ROS reduction. (A,B) RAW 264.7 macrophages were seeded at a density of 5×10^4 cells/mL and treated with FBCC-EP858 (100 μ g/mL), FBCC-EP920 (50 μ g/mL), and FBCC-EP1014 (100 μ g/mL) for 2 h followed by addition of 10 μ M ZnPP for 22 h. Then, 200 μ M hydrogen peroxide (H₂O₂) was treated for the last 4 h. (A) The cells were stained using a Muse Oxidative Stress Kit, and (B) ROS⁺ cell population was analyzed using a Muse Cell Analyzer. (C,D) The indicated concentration (50 μ g/mL) of FBCC-EP858, FBCC-EP920, and FBCC-EP1014 were treated to 3 dpf zebrafish larvae for 1 h followed by treatment with 10 μ M ZnPP for 1 h. Then, H₂O₂ (1 mM) was added for 22 h. (C) The larvae were stained using 20 μ M DCFDA for 30 min and visualized using a

CELENA S Digital Imaging System. (D) The DCFDA fluorescence intensity was calculated using ImageJ. Each value indicates the mean \pm SEM from three independent experiments. Significant difference: ### $p < 0.001$ vs. untreated group (Student's t -test), *** $p < 0.001$ vs. H₂O₂-treated group (one-way ANOVA), and +++ $p < 0.001$ vs. FBCCs + H₂O₂-treated group (one-way ANOVA).

4. Discussion

Oxidative stress is a condition that arises due to the imbalance between the production of ROS and the antioxidant defense system in the body. ROS can be generated endogenously during cellular metabolism or from exogenous sources such as exposure to cigarette smoke, ozone exposure, hypoxia, ionizing radiation, and heavy metal ions [37]. Oxidative stress has been implicated in various age-related and metabolic diseases, and targeting oxidative stress is a promising strategy for the prevention and treatment of this disease [1,38,39]. Antioxidant therapy, including plant-derived antioxidant agents, has been used in clinical trials due to its low toxicity and relevance to overall health and diseases [40]. In this study, we tested the DPPH radical scavenging activity of 184 plant extracts and identified three extracts (FBCC-EP858 from *A. multiflora*, FBCC-EP920 from *A. coccinea*, and FBCC-EP1014 from *S. gracilistyla*) that possessed powerful antioxidant activity. *A. multiflora*, *A. coccinea*, and *S. gracilistyla* are plants known for their traditional medicinal uses, and their antioxidant properties were previously unknown or not well-characterized [21,27]. We found that these extracts enhanced antioxidant activity both in vitro and in vivo by activating the Nrf2/HO-1 pathway. Overall, the study provides insight into the potential of plant-derived antioxidants as a therapeutic approach for oxidative stress-mediated human diseases.

Plant-derived natural antioxidants have been recognized as a potential therapeutic approach to reducing oxidative stress and associated diseases [17]. Cui et al. reported that plant-derived antioxidants protected the nervous system from aging by alleviating ROS production [41]. Akbarti et al. demonstrated that antioxidants supplied by foods or herbal supplements attenuated oxidative stress-associated chronic and degenerative diseases, such as cardiovascular, autoimmune, and neuronal diseases [42]. Additionally, the antioxidant properties of plant-derived compounds have received a great deal of attention in cosmetics because these antioxidants protect skin fibroblasts from ultraviolet-mediated ROS production and inhibit melanin biosynthesis [43,44]. In this regard, natural products targeting Nrf2 have received significant attention due to their potential to activate the antioxidant and detoxifying enzymes against oxidative stress and prevent ROS-mediated diseases such as inflammation, diabetes, and cancers [20,45]. In preclinical studies, some agents stimulating the Nrf2-HO-1 axis have shown promise in limiting inflammatory and oxidative stress biomarkers, and clinical trials in humans are underway [11]. The three powerful plant-derived antioxidant extracts (FBCC-EP858, FBCC-EP920, and FBCC-EP1014) identified in this study could potentially be used as antioxidant supplements due to their reported anti-inflammatory and antioxidant properties. Particularly, it was reported that *A. multiflora* contains anti-inflammatory and antioxidant compounds, such as rhamnetin and 3-rhamnosyl glucoside [26], and *A. coccinea* contains affluent flavonoid glycosides [46]. *S. gracilistyla* was proven to possess free radical scavenging and skin-whitening properties from the extracts of the stem [29]. Further analysis of the metabolites contained in each extract is necessary to identify their potential effects.

5. Conclusions

In conclusion, we selected three extracts with the strongest in vitro antioxidant activity from 184 plant extracts and verified their antioxidant properties on cells and zebrafish larvae. Furthermore, we confirmed that these three extracts exhibited powerful antioxidant effects through the activation of Nrf2 and HO-1. These findings suggest that three plant extracts have the potential as natural antioxidant supplements to prevent and treat various diseases caused by oxidative stress. Additionally, we conducted several bioactive assays on the extracts, revealing equivalent levels of antioxidant activity but differing levels of inhibition or activity in lipoxygenase, collagenase, α -glucosidase, acetaldehyde dehydrogenase, and

acetylcholine esterase (Supplementary Table S2). Further studies are needed to investigate the specific phytochemicals responsible for the antioxidant activity and to elucidate the molecular mechanisms underlying the protective effects of these extracts. Additionally, clinical trials are required to confirm their safety and efficacy in humans. Nevertheless, these results provide promising evidence for the potential of natural products as alternative sources of antioxidant therapy.

Supplementary Materials: The following supporting information can be downloaded at: <https://www.mdpi.com/article/10.3390/app13116701/s1>, Supplementary Table S1. FBCC code and plant sources used in this study and DPPH radical scavenging activity, Supplementary Table S2. In vitro enzyme inhibition (%) and activity (%) of three extracts used in this study.

Author Contributions: Conceptualization, J.A.C.C.J., M.-S.H. and G.-Y.K.; methodology, J.A.C.C.J., C.-H.K. and M.-H.L.; validation, J.A.C.C.J., C.-H.K., M.-H.L., Y.H.C. and M.-S.H.; resources, C.-H.K. and M.-H.L.; data curation, J.A.C.C.J., Y.H.C., M.-S.H. and G.-Y.K.; writing—original draft preparation, J.A.C.C.J.; writing—review and editing, Y.H.C., M.-S.H. and G.-Y.K.; supervision, G.-Y.K.; project administration, G.-Y.K. All authors have read and agreed to the published version of the manuscript.

Funding: This work was supported by the Korea Environment, Industry & Technology Institute (KEITI) through the Project to Make Multi-ministerial National Biological Research Resources More Advanced, funded by the Korea Ministry of Environment (MOE) (No. 2021003420002).

Institutional Review Board Statement: Animal experiments were carried out after approval (Approval No. 2022-0084) from the Institutional Animal Care and Use Committee of Jeju National University (Jeju, Republic of Korea).

Data Availability Statement: All data can be obtained from the corresponding authors upon a rational request.

Conflicts of Interest: The authors declare no potential conflict of interest.

References

1. Koutsaliaris, I.K.; Moschonas, I.C.; Pechlivani, L.M.; Tsouka, A.N.; Tselepis, A.D. Inflammation, oxidative stress, vascular aging and atherosclerotic ischemic stroke. *Curr. Med. Chem.* **2022**, *29*, 5496–5509.
2. Azmanova, M.; Pitto-Barry, A. Oxidative stress in cancer therapy: Friend or enemy? *Chembiochem* **2022**, *23*, e202100641. [[CrossRef](#)]
3. Juan, C.A.; Perez de la Lastra, J.M.; Plou, F.J.; Perez-Lebena, E. The chemistry of reactive oxygen species (ROS) revisited: Outlining their role in biological macromolecules (DNA, lipids and proteins) and induced pathologies. *Int. J. Mol. Sci.* **2021**, *22*, 4642. [[CrossRef](#)] [[PubMed](#)]
4. Su, L.J.; Zhang, J.H.; Gomez, H.; Murugan, R.; Hong, X.; Xu, D.; Jiang, F.; Peng, Z.Y. Reactive oxygen species-induced lipid peroxidation in apoptosis, autophagy, and ferroptosis. *Oxid. Med. Cell. Longev.* **2019**, *2019*, 5080843. [[CrossRef](#)] [[PubMed](#)]
5. Checa, J.; Aran, J.M. Reactive oxygen species: Drivers of physiological and pathological processes. *J. Inflamm. Res.* **2020**, *13*, 1057–1073. [[CrossRef](#)] [[PubMed](#)]
6. He, L.; He, T.; Farrar, S.; Ji, L.; Liu, T.; Ma, X. Antioxidants maintain cellular redox homeostasis by elimination of reactive oxygen species. *Cell. Physiol. Biochem.* **2017**, *44*, 532–553. [[CrossRef](#)] [[PubMed](#)]
7. Liu, S.; Pi, J.; Zhang, Q. Signal amplification in the KEAP1-NRF2-ARE antioxidant response pathway. *Redox Biol.* **2022**, *54*, 102389. [[CrossRef](#)]
8. Nguyen, T.; Nioi, P.; Pickett, C.B. The Nrf2-antioxidant response element signaling pathway and its activation by oxidative stress. *J. Biol. Chem.* **2009**, *284*, 13291–13295. [[CrossRef](#)]
9. Motohashi, H.; Yamamoto, M. Nrf2–Keap1 defines a physiologically important stress response mechanism. *Trends Mol. Med.* **2004**, *10*, 549–557. [[CrossRef](#)]
10. Loboda, A.; Damulewicz, M.; Pyza, E.; Jozkowicz, A.; Dulak, J. Role of Nrf2/HO-1 system in development, oxidative stress response and diseases: An evolutionarily conserved mechanism. *Cell. Mol. Life Sci.* **2016**, *73*, 3221–3247. [[CrossRef](#)]
11. Yagishita, Y.; Gatbonton-Schwager, T.N.; McCallum, M.L.; Kensler, T.W. Current landscape of NRF2 biomarkers in clinical trials. *Antioxidants* **2020**, *9*, 716. [[CrossRef](#)] [[PubMed](#)]
12. Zhai, Z.; Huang, Y.; Zhang, Y.; Zhao, L.; Li, W. Clinical research progress of small molecule compounds targeting Nrf2 for treating inflammation-related diseases. *Antioxidants* **2022**, *11*, 1564. [[CrossRef](#)] [[PubMed](#)]
13. Marzioni, D.; Mazzucchelli, R.; Fantone, S.; Tossetta, G. NRF2 modulation in TRAMP mice: An in vivo model of prostate cancer. *Mol. Biol. Rep.* **2023**, *50*, 873–881. [[CrossRef](#)] [[PubMed](#)]
14. Saw, C.L.; Kong, A.N. Nuclear factor-erythroid 2-related factor 2 as a chemopreventive target in colorectal cancer. *Expert Opin. Ther. Targets* **2011**, *15*, 281–295. [[CrossRef](#)]

15. Wang, P.; Long, F.; Lin, H.; Wang, T. Dietary phytochemicals targeting Nrf2 for chemoprevention in breast cancer. *Food Funct.* **2022**, *13*, 4273–4285. [[CrossRef](#)]
16. Samtiya, M.; Aluko, R.E.; Dhewa, T.; Moreno-Rojas, J.M. Potential health benefits of plant food-derived bioactive components: An overview. *Foods* **2021**, *10*, 839. [[CrossRef](#)]
17. Szymanska, R.; Pospisil, P.; Kruk, J. Plant-derived antioxidants in disease prevention. *Oxid. Med. Cell. Longev.* **2016**, *2016*, 1920208. [[CrossRef](#)]
18. Kasote, D.M.; Katyare, S.S.; Hegde, M.V.; Bae, H. Significance of antioxidant potential of plants and its relevance to therapeutic applications. *Int. J. Biol. Sci.* **2015**, *11*, 982–991. [[CrossRef](#)]
19. Abbate, F.; Maugeri, A.; Laurà, R.; Levanti, M.; Navarra, M.; Cirmi, S.; Germanà, A. Zebrafish as a useful model to study oxidative stress-linked disorders: Focus on flavonoids. *Antioxidants* **2021**, *10*, 668. [[CrossRef](#)]
20. Kumar, H.; Kim, I.S.; More, S.V.; Kim, B.W.; Choi, D.K. Natural product-derived pharmacological modulators of Nrf2/ARE pathway for chronic diseases. *Nat. Prod. Rep.* **2014**, *31*, 109–139. [[CrossRef](#)]
21. Deng, W.; Duan, Z.; Li, Y.; Cui, H.; Peng, C.; Yuan, S. Characterization of target-site resistance to ALS-inhibiting herbicides in *Ammannia multiflora* populations. *Weed Sci.* **2022**, *70*, 292–297. [[CrossRef](#)]
22. Upadhyay, H.C.; Dwivedi, G.R.; Darokar, M.P.; Chaturvedi, V.; Srivastava, S.K. Bioenhancing and antimycobacterial agents from *Ammannia multiflora*. *Planta Med.* **2012**, *78*, 79–81. [[CrossRef](#)]
23. Upadhyay, H.C.; Sisodia, B.S.; Agrawal, J.; Pal, A.; Darokar, M.P.; Srivastava, S.K. Antimalarial potential of extracts and isolated compounds from four species of genus *Ammannia*. *Med. Chem. Res.* **2014**, *23*, 870–876. [[CrossRef](#)]
24. Upadhyay, H.C.; Jaiswal, N.; Tamrakar, A.K.; Srivastava, A.K.; Gupta, N.; Srivastava, S.K. Antihyperglycemic agents from *Ammannia multiflora*. *Nat. Prod. Commun.* **2012**, *7*, 899–900. [[CrossRef](#)] [[PubMed](#)]
25. Upadhyay, H.C. Medicinal chemistry of alternative therapeutics: Novelty and hopes with genus *Ammannia*. *Curr. Top. Med. Chem.* **2019**, *19*, 784–794. [[CrossRef](#)]
26. Upadhyay, H.; Saini, D.; Srivastava, S. Phytochemical analysis of *Ammannia multiflora*. *Res. J. Phytochem.* **2011**, *5*, 170–176.
27. Naqinezhad, A.; Larijani, N.N. *Ammannia coccinea* (Lythraceae), a new record for the Flora Iranica area. *Phytol. Balca.* **2017**, *23*, 35–38.
28. Jarolimek, I.; Kolbek, J. Plant communities dominated by *Salix gracilistyla* in Korean Peninsula and Japan. *Biologia* **2006**, *61*, 63–70. [[CrossRef](#)]
29. Jeong, Y.-U.; Park, Y.-J. Studies on antioxidant and whitening activities of *Salix gracilistyla* extracts. *J. Soc. Cosmet. Sci. Korea* **2018**, *44*, 317–325.
30. Sales, P.M.; Souza, P.M.; Simeoni, L.A.; Magalhães, P.O.; Silveira, D. α -Amylase inhibitors: A review of raw material and isolated compounds from plant source. *J. Pharm. Pharm. Sci.* **2012**, *15*, 141–183. [[CrossRef](#)]
31. Molagoda, I.M.; Lee, K.T.; Choi, Y.H.; Kim, G.-Y. Anthocyanins from *Hibiscus syriacus* L. inhibit oxidative stress-mediated apoptosis by activating the Nrf2/HO-1 signaling pathway. *Antioxidants* **2020**, *9*, 42. [[CrossRef](#)] [[PubMed](#)]
32. Molagoda, I.M.; Athapaththu, A.M.; Choi, Y.H.; Park, C.; Jin, C.-Y.; Kang, C.-H.; Lee, M.-H.; Kim, G.-Y. Fisetin inhibits NLRP3 inflammasome by suppressing TLR4/MD2-mediated mitochondrial ROS production. *Antioxidants* **2021**, *10*, 1215. [[CrossRef](#)] [[PubMed](#)]
33. Jayasingha, J.; Lee, K.; Choi, Y.; Kang, C.-H.; Lee, M.-H.; Kim, G.-Y. Aqueous extract of freeze-dried *Protaetia brevitarsis* larvae promotes osteogenesis by activating β -catenin signaling. *Asian Pac. J. Trop. Biomed.* **2022**, *12*, 115–123.
34. Molagoda, I.M.N.; Kang, C.-H.; Lee, M.-H.; Choi, Y.H.; Lee, C.-M.; Lee, S.; Kim, G.-Y. Fisetin promotes osteoblast differentiation and osteogenesis through GSK-3 β phosphorylation at Ser9 and consequent β -catenin activation, inhibiting osteoporosis. *Biochem. Pharmacol.* **2021**, *192*, 114676. [[CrossRef](#)] [[PubMed](#)]
35. Alestrom, P.; D'Angelo, L.; Midtlyng, P.J.; Schorderet, D.F.; Schulte-Merker, S.; Sohm, F.; Warner, S. Zebrafish: Housing and husbandry recommendations. *Lab. Anim.* **2020**, *54*, 213–224. [[CrossRef](#)] [[PubMed](#)]
36. Suski, J.M.; Lebieczinska, M.; Bonora, M.; Pinton, P.; Duszynski, J.; Wieckowski, M.R. Relation between mitochondrial membrane potential and ROS formation. *Methods Mol. Biol.* **2012**, *810*, 183–205.
37. Sies, H.; Berndt, C.; Jones, D.P. Oxidative stress. *Annu. Rev. Biochem.* **2017**, *86*, 715–748. [[CrossRef](#)]
38. Cabello-Verrugio, C.; Simon, F.; Trollet, C.; Santibanez, J.F. Oxidative stress in disease and aging: Mechanisms and therapies 2016. *Oxid. Med. Cell. Longev.* **2017**, *2017*, 4310469. [[CrossRef](#)]
39. Luo, J.; Mills, K.; le Cessie, S.; Noordam, R.; van Heemst, D. Ageing, age-related diseases and oxidative stress: What to do next? *Ageing Res. Rev.* **2020**, *57*, 100982. [[CrossRef](#)]
40. Pandey, K.B.; Rizvi, S.I. Plant polyphenols as dietary antioxidants in human health and disease. *Oxid. Med. Cell. Longev.* **2009**, *2*, 270–278. [[CrossRef](#)]
41. Cui, X.; Lin, Q.; Liang, Y. Plant-derived antioxidants protect the nervous system from aging by inhibiting oxidative stress. *Front. Aging Neurosci.* **2020**, *12*, 209. [[CrossRef](#)] [[PubMed](#)]
42. Akbari, B.; Baghaei-Yazdi, N.; Bahmaie, M.; Mahdavi Abhari, F. The role of plant-derived natural antioxidants in reduction of oxidative stress. *Biofactors* **2022**, *48*, 611–633. [[CrossRef](#)] [[PubMed](#)]
43. Merez-Sadowska, A.; Sitarek, P.; Kucharska, E.; Kowalczyk, T.; Zajdel, K.; Ceglinski, T.; Zajdel, R. Antioxidant properties of plant-derived phenolic compounds and their effect on skin fibroblast cells. *Antioxidants* **2021**, *10*, 726. [[CrossRef](#)] [[PubMed](#)]

44. Michalak, M. Plant-derived antioxidants: Significance in skin health and the ageing process. *Int. J. Mol. Sci.* **2022**, *23*, 585. [[CrossRef](#)]
45. Zhang, Y.; Wang, B.; Lu, F.; Wang, L.; Ding, Y.; Kang, X. Plant-derived antioxidants incorporated into active packaging intended for vegetables and fatty animal products: A review. *Food Addit. Contam. Part A* **2021**, *38*, 1237–1248. [[CrossRef](#)]
46. Graham, S.A.; Timmermann, B.N.; Mabry, T.J. Flavonoid glycosides in *Ammannia coccinea* (Lythraceae). *J. Nat. Prod.* **1980**, *43*, 644–645. [[CrossRef](#)]

Disclaimer/Publisher's Note: The statements, opinions and data contained in all publications are solely those of the individual author(s) and contributor(s) and not of MDPI and/or the editor(s). MDPI and/or the editor(s) disclaim responsibility for any injury to people or property resulting from any ideas, methods, instructions or products referred to in the content.